E. ATTRIBUTION OF 2012 AND 2003–12 RAINFALL DEFICITS IN EASTERN KENYA AND SOUTHERN SOMALIA

Chris Funk, Greg Husak, Joel Michaelsen, Shraddhanand Shukla, Andrew Hoell, Bradfield Lyon, Martin P. Hoerling, Brant Liebmann, Tao Zhang, James Verdin, Gideon Galu, Gary Eilerts, and James Rowland

Introduction. Over the past 14 years, eastern East Africa has experienced more frequent boreal spring dry events (Funk et al. 2008; Williams and Funk 2011; Lyon and DeWitt 2012; Funk 2012). In the spring of 2012, below-average March–May rains across parts of eastern Kenya and Southern Somalia (a region bounded by 4°S–4°N, 37°E–43°E, green polygon, Fig. E1A) once again contributed to crisis and emergency levels of food insecurity (FEWS NET 2012a). In some regions, rainfall deficits of more than 30% led to crop failures and poor pasture conditions, causing families in Kenya to move in search of work or take children out of school, and inhibiting Somalia's recovery from the acute malnutrition and famine caused by the 2010–11 drought. While not particularly severe, the poor March–May 2012 rains added to climatic stresses associated with a series of March–May dry events occurring in 2007, 2008, 2009, and 2011. Figure E1b shows March–May (three month) Standardized Precipitation Index (SPI; McKee et al. 1993) values, based on 1981–2012 FEWS NET precipitation data (see Supplemental Material for a brief description). Dry events, defined as March–May seasons with SPI values of less than -0.5, are shown in orange. In fragile food economies, these repetitive dry events can lower resilience, disrupt development, and require large infusions of emergency assistance. It is not the climate alone that creates these outcomes, but rather the climate's interaction with extreme poverty, high-endemic rates of malnutrition, limited or nonexistent governmental safety nets, and poor governance. In 2011, for example, the worst drought in 60 years combined with chronic food insecurity, high global food prices, and the actions of Somali terrorists produced an estimated 258 000 deaths in Somalia (FEWS NET, 2013).

In this study, we examine the question of whether sea surface temperatures (SSTs) caused the poor 2012 March–May eastern East African rains and increased the frequency of dry events over the past decade (2003–12), using two new Global Forecast System

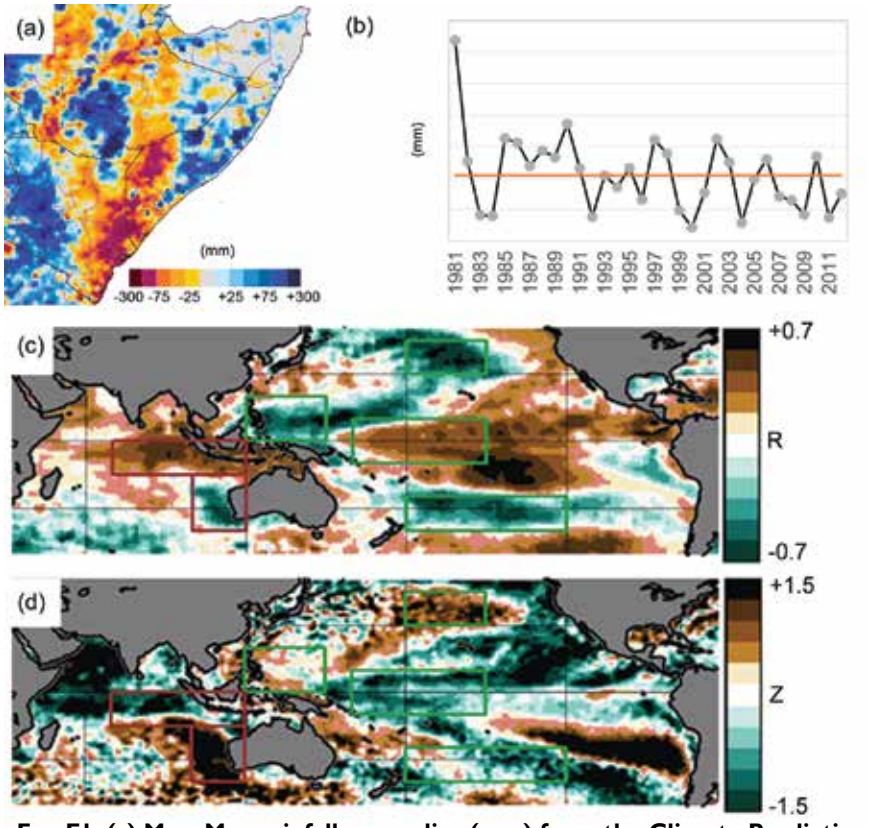

Fig. E1. (a) Mar–May rainfall anomalies (mm) from the Climate Prediction Center's RFE2 dataset. (b) 1981–2012 time series of EA rainfall (mm) based on blended infrared observations, the CFS reanalysis, and station data. (c) 1999–2012 correlations between EA SPI and Mar SSTs. (d) Observed (NOAA AVHRR OI) Mar SST anomalies.

(Environmental Modeling Center 2003) version 2 (GFS) ensembles to estimate fractions of attributable risk (FAR; Allen 2003) associated with 30 full-ocean simulations and 30 simulations driven only with detrended El Niño-Southern Oscillation (ENSO-only) SSTs.

The approach taken here is somewhat similar to the attribution study of Lott et al. (2013), which focused on the 2010 and 2011 East African droughts, except that where Lott et al. (2013) contrast full-ocean and "natural" SST influences, we examine the differences between full-ocean and ENSO-only SST effects. Lott el al. (2013) drove a state-of-the-art atmosphere model with observed (full-ocean) and "natural" SSTs. "Natural" SSTs were observed SSTs with estimates of anthropogenic warming removed. Ensembles of full and natural precipitation ensembles were compared, and the fraction of attributable drought risk (Allen 2003) estimated ($FAR = 1.0 - PROB_{nat}/PROB_{full}$). Lott el al. (2013) found that the risk of the 2011 spring drought, but not the 2010 ENSO-related fall drought, increased substantially; a result consistent with a recent regional modeling study by Cook and Vizy (2013), which found that during the 21st century, anomalous dry anticyclonic flow from the Arabian peninsula reduced boreal spring rains, while boreal winter rains are lengthened by a northeastward shift of the South Indian convergence zone.

Rather than comparing "natural" and full-ocean results, here we present an analysis contrasting full-ocean and ENSO-only simulations. We examine FAR values based on the full-ocean and ENSO-only simulations: $FAR = 1.0 - PROB_{ENSO}/PROB_{full}$. Full-ocean GFS simulations were driven with observed SSTs and atmospheric carbon dioxide variability. ENSO-only simulations were driven with de-trended SST variations associated with the first principal component of Pacific SSTs and atmospheric carbon dioxide variability. Comparisons of these simulations allow us to examine whether recent dry events have likely been due to La Niña-like anomalies (Ogallo 1988) or other SST changes, potentially related to warming in the Indo-Pacific. The full-ocean and ENSO-only ensembles are based on T126 spectral resolution GFS precipitation simulations.

2012 SST conditions. Our understanding of the sea surface and climate conditions underpinning recent East African (EA) dry events is growing rapidly. The most recent (21st century) increase in March–May EA dry event frequency appears related to Indo-Pacific warming (Funk et al. 2008; Williams and Funk 2011; Funk 2012), a stronger western-to-central Pacific SST gradient (Lyon and DeWitt 2012), and an intensification of the Walker circulation (Hoerling et al. 2010; Williams and Funk 2011; Merrifield and Maltrud 2011; Meng et al. 2012; L'Heureux et al. 2013). When the Central Pacific is cool and the Western Pacific warm, a vigorous circulation response (Hoerling and Kumar 2002; Hoerling and Kumar 2003) increases rainfall over the eastern Indian and western Pacific oceans but can reduce rainfall over eastern Africa and other teleconnected regions, such as southwest Asia (Hoell and Funk 2013). Standardized equatorial Indo-Pacific SST transects for dry events (Supplementary Fig. ES1a) associate below-normal EA rainfall with stronger western-to-eastern Pacific SST gradients.

Correlations between 1993–2012 March–May EA SPI and March SSTs (Fig. E1c) indicate fairly strong teleconnections. Warm SSTs in the Western Pacific combined with cool SSTs in the central Indian Ocean and central Pacific tend to produce drier-than-normal rainfall in eastern East Africa.

In March of 2012, the East African food security was tenuous, and the March SST anomalies (Fig. E1D) exhibited anomalies congruent with below normal rains. Indices based on teleconnected regions were used to define analogs to the observed 2012 March SSTs, and below-normal rainfall was anticipated by FEWS NET (2012a). These results were similar to forecast outlooks produced by African experts at the 30th Greater Horn of Africa Climate Outlook Forum (GHACOF 2012) and bias corrected ECHAM4.5 rainfall forecasts provided by the IRI. The FEWS NET, GHACOF, and IRI outlooks all indicated below-normal rains. On 3 April, FEWS NET (2012b) released a forecast of below-normal precipitation. On 5 April, the State Department announced an increase in humanitarian assistance (State Department 2012). In June, prepositioned resources and contingency planning helped mitigate crisis-level food insecurity conditions (FEWS NET 2012b).

Attribution of the 2012 East African dry event. In the results presented here, we use a simple regression (see Supplemental Material for more details) between 1993–2012 EA SPI values and GFS precipitation over the western Pacific (0°–20°N, 120°E–160°E) to estimate EA precipitation conditions. This approach was taken because (i) the correlation between local EA SPI and the EA GFS precipitation was low ($r = 0.34$, df. 18, $p = 0.08$), while the anti-correlation to western Pacific precipitation was fairly strong (-0.71), and (ii) the intensity of convection in the equatorial western Pacific has been linked to recent EA dry events (Lyon and DeWitt 2012; Williams and Funk 2011).

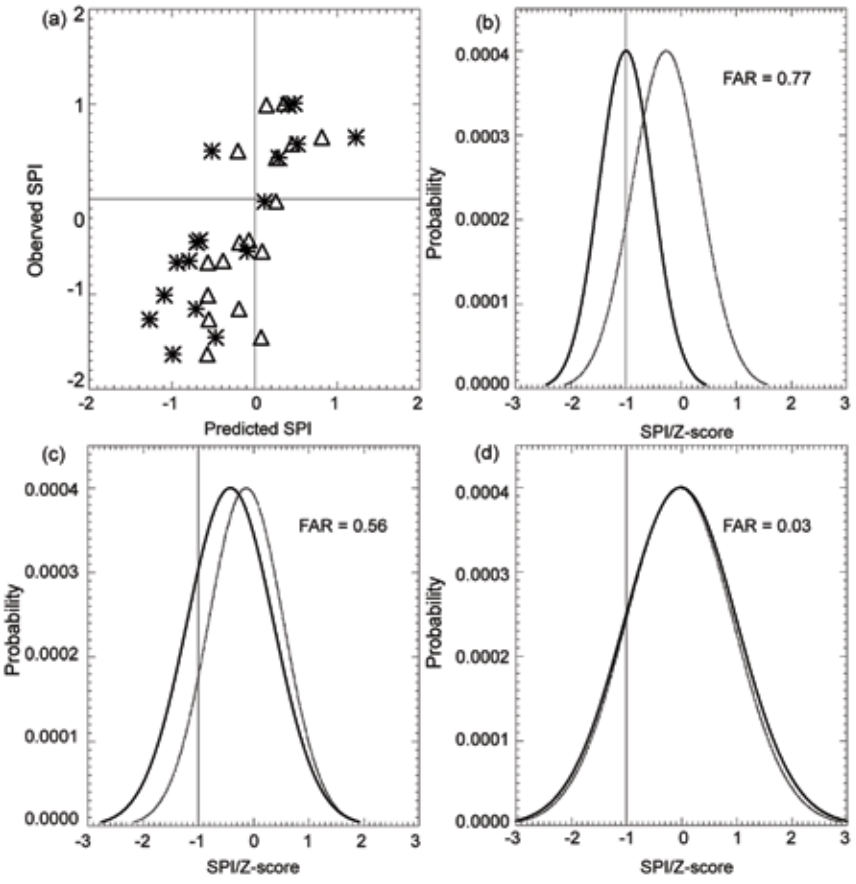

Fig. E2. (a) Predicted and observed EA SPI values for the full-ocean GFS (*) and ENSO-only GFS (Δ). (b) 2012 EA SPI probability distributions for the full-ocean GFS predictions (solid line) and ENSO-only predictions (dashed line). (c) Same as (b) but calculated over 2003–12. (d) Same as (b) but calculated over 1993–2002.

The results presented here indicate that both ENSO and non-ENSO SST variations played some role in forcing the 1993–2012 EA SPI, but that non-ENSO forcing dominated during the 2012 boreal spring. The scatterplot shown in Fig. E2a shows the ensemble mean full-ocean and ENSO-only estimate, indicated respectively with * and Δ. Between 1993 and 2012, the cross-validated full-ocean estimates explained 50% of the variance of the observed rainfall and captured many of the recent dry events. The ENSO-only estimates, however, failed to recreate the observed dry event intensities. The ENSO-only estimates also missed dry events in 2004 and 2012 that were captured in the full-ocean simulations. The full-ocean and ENSO estimates are correlated at 0.74, but the standard deviation of the full-ocean estimates are 25% greater. Figure E2b shows a comparison of the full-ocean and ENSO-only estimates. During years with suppressed western Pacific precipitation and normal-to-above-normal EA SPI estimates, the two ensembles track closely. In seasons with above normal western Pacific precipitation and below-normal EA SPI estimates, the agreement is weaker, and the full-ocean estimates of EA SPI are lower. This may indicate substantial forcing by non-ENSO sources.

Ensembles of downscaled full-ocean and ENSO-only SPI estimates can be used to calculate the 2012 dry event FAR (Allen 2003). FAR measures how much more likely an event is, given a change in the climate system. The two sets of ensembles define two probability distributions, and FAR is calculated based on their differences. Figure E2c shows the distributions of the 2012 full-ocean and ENSO-only estimated SPI ensembles. The full-ocean (ENSO-only) predictions had a mean and standard deviation of -1.0 and 0.6 (-0.1 and 0.4). Defining a dry event as having an SPI value of -0.5 or less, we find that dry events were much more likely (85% probability) in the full-ocean than in the ENSO-only simulations (18% probability) yielding a $F_{AR} = 1.0 - P_{ENSO}/P_{FULL} = 0.85$. Non-ENSO SSTs appear to have substantially increased the risk of a dry event in 2012.

Attribution of the 2003–12 and 1993–2002 East African dry events. We can apply the same FAR analysis technique to all GFS estimates for the past ten years (2003–12). The mean and standard deviation of the 300 full-ocean simulations (10 seasons with 30 simulations) was -0.3 and 0.7. The corresponding mean and standard deviation for the 300 ENSO-only simulations was -0.1 and 0.6. Over this decade, the full-ocean simulations indicated a 42% chance of dry events (SPI < -0.5), while the ENSO-only simulations indicated a 27% chance. These frequencies correspond to a dry event every 2.4 and 3.7 years. The corresponding FAR value is 0.37 (Fig. E2d), signifying that non-ENSO SST variations have made dry events more likely. A similar analysis is also shown for the 1993–2002 period (Fig. E2d). In this decade, the probability of dry events was similar in the full-

ocean and ENSO-only ensembles (~30%). Together, the 1993–2002 and 2003–12 results suggest the recent emergence of a non-ENSO driven dry event forcing.

Conclusion. The results indicate that non-ENSO SST variations substantially increased the risk of a dry event in 2012, and over the 2003–12 period. ENSO SST conditions cannot fully account for the recent increase in eastern East African dry event frequencies. It seems likely that other factors, such as warming in the western Pacific (Williams and Funk 2011; Lyon and DeWitt 2012; Funk 2012), a recent transition in Pacific decadal variability (Gu and Adler 2013), and stronger western-to-central Pacific SST gradients (Hoell and Funk 2013) may be contributing to the recent dryness. On the other hand, it is also important to recognize that the results indicate that ENSO has had substantial links to recent EA precipitation variations.

It is worth noting, however, that the procedure used here does not necessarily indicate an anthropogenic attribution since we are comparing the full SST results with ENSO-only SSTs, rather than estimates of "natural" SSTs as in Lott et al. (2013). Observed western Pacific and eastern Indian Ocean SSTs do, however, track very closely with historical simulations from coupled ocean-atmosphere climate change models (Funk 2012), and this region has been warming substantially faster than the eastern Pacific (Cane et al. 1997; Compo and Sardeshmukh 2010; Lott et al. 2013; Solomon and Newman 2012) in a manner that may be consistent with a stronger radiative control of the western versus eastern Pacific (Clement et al. 1996). Recent studies using paleoclimate data associate such warming with East African drying (Tierney et al. 2013), and more trend analyses are identifying recent rainfall declines (Viste et al. 2012). On the other hand, coupled ocean-atmosphere climate change models tend to indicate a tendency for wetter conditions in eastern Africa. Finally, Pacific decadal variations have also likely played an important role, triggering a post-1998 climate shift (Gu and Adler 2013) that enhanced tropical Pacific precipitation and SST gradients.